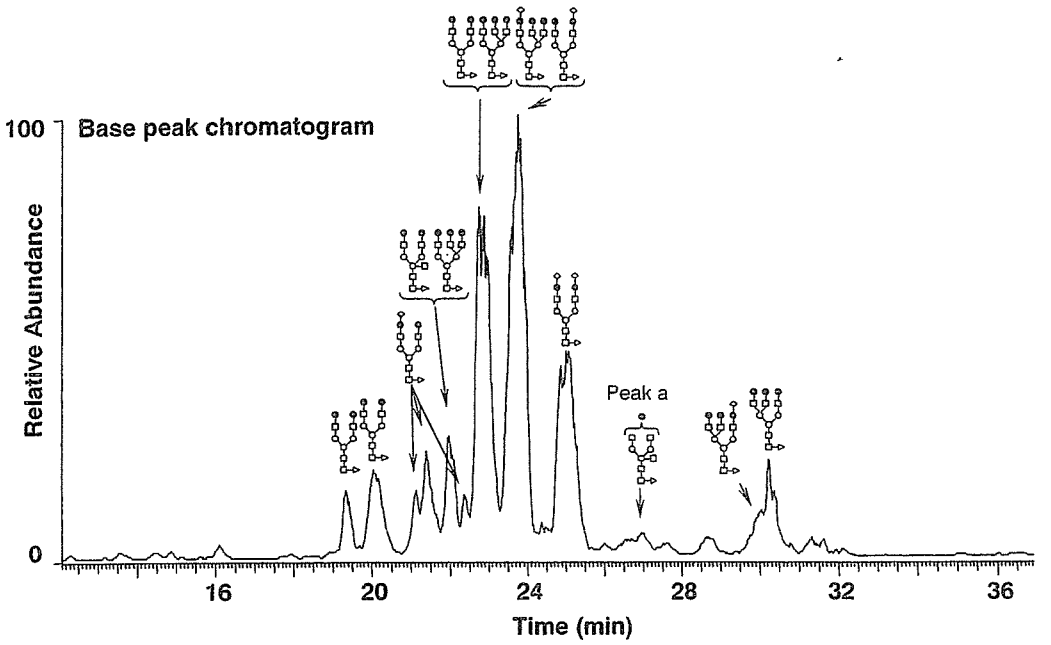

Fig. 7　GnT-III 遺伝子導入 CHO 細胞で発現させた糖鎖改変型フォリスタチン由来 PA 化糖鎖の LC/MS^1 によって得られたベースピーククロマトグラム

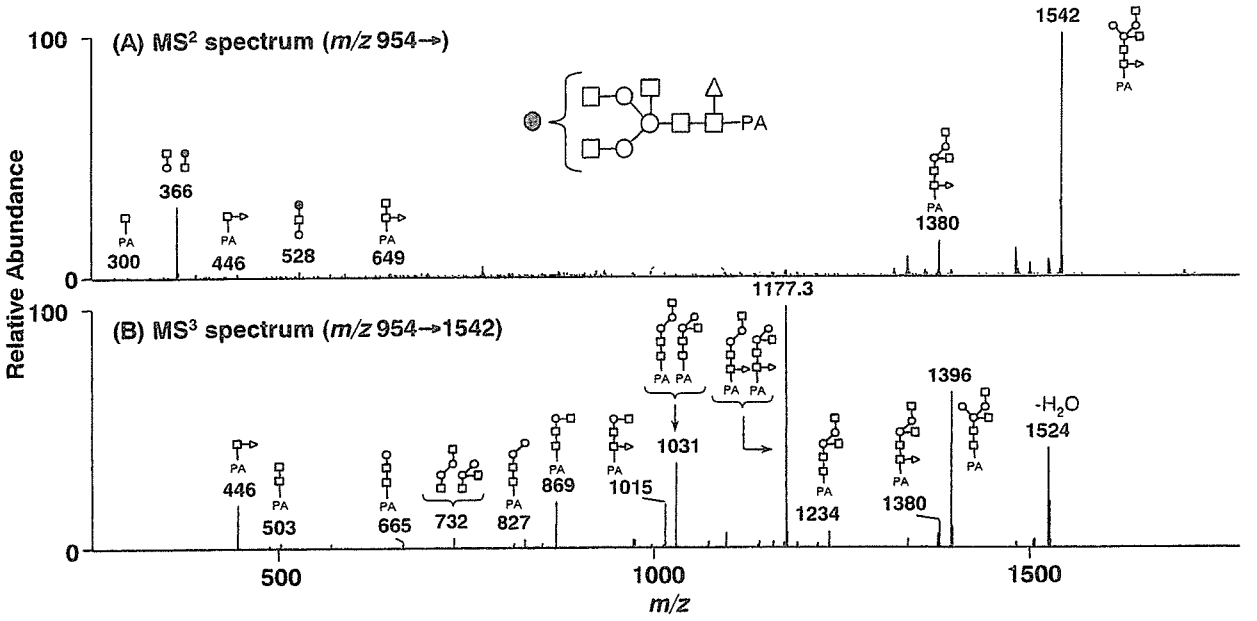

Fig. 8　Fig. 7 中のピーク a の代表的 MS^{2,3} スペクトル
(A) MS^2 スペクトル　前駆イオン：m/z 954, ポジティブイオンモード
(B) MS^3 スペクトル　前駆イオン：m/z 1542, ポジティブイオンモード

文　献

1) Varki, A.: *Glycobiology*, **3**, 97-130 (1993).
2) Kawasaki, N., Ohta, M., Hyuga, S., Hyuga, M., Hayakawa, T.: *Anal. Biochem.*, **285**, 82-91 (2000).
3) Kawasaki, N., Itoh, S., Ohta, M., Hayakawa, T.: *Anal. Biochem.*, **316**, 15-22 (2003).
4) Itoh, S., Kawasaki, N., Ohta, M., Hyuga, M., Hyuga, S., Hayakawa, T.: *J. Chromatogr, A*, **978**, 141-152 (2002).
5) Kobata, A.: *J. Cell Biochem.*, **37**, 79-90 (1988).
6) Hase, S., Ibuki, T., Ikenaka, T.: *J. Biochem.*, **95**, 197-203 (1984).
7) Tomiya, N., Kurono, M., Ishihara, H., Tejima, S., Endo, S., Arata, Y., Takahashi, N.: *Anal. Biochem.*, **163**, 489-499 (1987).
8) Nakamura, T., Takio, K., Eto, Y., Shidai, H., Titani, K., Sugino, H.: *Science*, **247**, 836-838 (1990).
9) Hyuga, M., Itoh, S., Kawasaki, N., Ohta, M., Ishii, A., Hyuga, S., Hayakawa, T.: *Biologicals*, **32**, 70-77 (2004).

細胞治療薬の品質・安全性評価における糖鎖解析の重要性とLC/MSの応用可能性

川崎 ナナ、橋井 則貴、伊藤 さつき、山口 照英
(国立医薬品食品衛生研究所 生物薬品部)

はじめに

ヒトまたは動物より分離した細胞や組織を培養、加工し、直接患者に投与することにより、様々な疾患を治療する細胞治療/再生医療が著しい進展を遂げている。この細胞治療/再生医療の開発には大きく分けて、2つの流れがある。一つは医療行為としての細胞治療/再生医療技術の開発で、我が国の医療機関における細胞治療/再生医療の臨床応用は200例を超えている。もう一つは、薬事法上の規制を受ける細胞治療薬(細胞組織利用医薬品)の開発である。細胞治療薬 (cell therapy products)とは、細胞治療を目的として、自己、同種、あるいは異種の細胞を生体外で選別し、加工し、あるいは増殖した後にヒトに投与する医薬品のことで、近年、細胞治療薬の開発は企業活動として活発化してきた。今後の本格的な実用化に向けて、現在、細胞治療薬の有効性確保と特性解析及び品質・安全性評価技術の開発が求められている。

厚生労働省は、細胞治療薬に関連して表1に示す指針や通知を出している。細胞治療薬の品質及び安全性の確保に関する基本的な考え方は、医薬発第1314号に示されている。表2は医薬発第1314号に記載されている品質・安全性確保のための製造工程及び最終製品レベルの規格及び試験法に関する事項の要点をまとめたものである。この中の同一性、細胞由来生理活性物質、製造工程由来不純物、細胞の純度、及び細胞由来目的外生理活性物質の確認に対しては、その規格及び試験法の一般化・標準化を目的として、様々な方法が検討されている。現在、染色体、遺伝子、タンパク質レベルでの解析が検討されているが、細胞分化や機能発現に糖鎖が重要な役割を果たしていることが明らかになってきていることを考慮すると、糖鎖構造に着目した品質・安全性評価法の有用性評価が必要になってくると思われる。

糖鎖解析法として、液体クロマトグラフィー(LC)、キャピラリー電気泳動法、質量分析法(MS)、及びレクチンを用いた方法等、多くの優れた方法が報告されている。しかし、これらを

表1.

我が国における細胞治療薬に関連する指針や通知

- 細胞・組織利用医薬品等の品質及び安全性の確保について(医薬発第906号)
- 細胞・組織利用医薬品等の取扱い及び使用に関する基本的考え方(医薬発第1314号)
- ヒト由来細胞・組織加工医薬品等の品質及び安全性の確保に関する指針(医薬発第1314号)
- 生物由来製品及び特定生物由来製品の指定並びに生物由来原料基準の制定等について(医薬発第052001号)
- 生物由来製品に関する感染症定期報告制度について(医薬発第051508号)

表2.

製造工程及び最終製品レベルの規格・試験方法

- 回収率や生存率
- 同一性の確認
- 細胞由来生理活性物質(必要に応じて)
- 無菌試験、マイコプラズマ試験
- エンドトキシン試験
- 製造工程由来不純物試験
- 細胞の純度試験
- 細胞由来目的外生理活性物質
- ウイルス等の試験

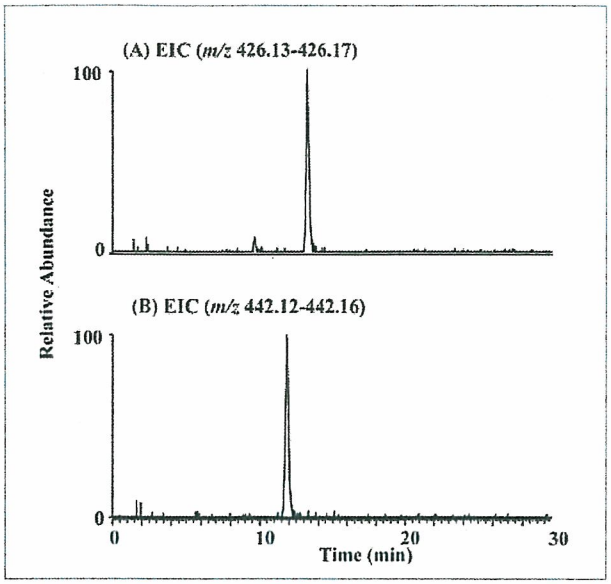

図1．DMB誘導体化シアル酸のLC/FTMS
(A) m/z 426.13-426.17(DMB-NeuAc)のマスクロマトグラム
(B) m/z 442.12-442.16 (DMB-NeuGc)のマスクロマトグラム

FCS、ヒト血清、及び無血清培地で培養したHL-60細胞 (2.5 x 10^5個) の膜画分に存在するシアル酸含量

	NeuAc (pmol±SD)	NeuGc (pmol±SD)	NeuGc/NeuAc (%)
FCS	13.5±0.6	0.055±0.0046	0.41
ヒト血清	21.0±1.4	0.029±0.0024	0.14
無血清	20.5±1.6	N.D.	

表3.

細胞治療薬の品質・安全性評価に応用するには大きな課題がある。それは、細胞治療薬の品質・安全性試験に使用できる細胞数は限られているということである。検体となる細胞の数は、細胞の性質にも依存するが、自己由来細胞で10^6個、また同種由来細胞で10^8個程度と推定されている。従って、従来の分析法を試験法として利用するには、感度及び選択性の向上が要求される。国立医薬品食品衛生研究所では、感度と選択性に優れ、一度に多くの情報を得られるnanoLC/MSを細胞治療薬の品質・安全性評価に利用することを検討してきた。本稿ではその一部を紹介する。

1．製造工程由来不純物試験

製造工程由来不純物とは、医薬品製造中に血清、培地、及び試薬等から混入し、品質・有効性・安全性に影響を及ぼすおそれがある物質のことで、最終製品中に含まれる対象分子の定量試験を設定し、存在を否定するか、もしくは予め規定した存在許容量以下であることを確認する必要がある。現在、製造工程において血清やフィーダー細胞から混入されることが懸念されている物質の一つに、シアル酸の一種である*N*-グリコリルノイラミン酸(NeuGc)がある。NeuGcは、ウシなど様々な動物で産生されるが、ヒトでは産生されないために、ヒトに対して抗原性を示すことが知られている[1]。2005年Martinら[2]によって、ヒト胚性幹細胞(ES細胞)培養過程で、異種血清やフィーダー細胞からNeuGcが混入することが報告されて以来、NeuGcが細胞治療薬の有効性や安全性へ及ぼす影響が懸念されるようになってきた。

有効性や安全性への影響を評価するにあたって、まず、細胞治療薬に含まれるNeuGcの量を正確に測定する必要がある。細胞中のシアル酸の定量法として、1,2-diamino-4,5-methylenedioxybenzene (DMB)誘導体化とLC/蛍光検出法(FD)を組み合わせた方法がよく用いられている[3]。DMB誘導体化とLC/FDにMS及びMS/MSを組み合わせると、分子量やフラグメントからシアル酸分子種を確認することができる[4]。しかし、既存の分析法の検出感度 (検出限界5 pmol)は、細胞治療薬の品質評価法としては十分ではなく、分析の微量化が求められる。

我々は、nanoLC/フーリエ変換イオンサイクロトロン共鳴質量分析法(FTMS)及びnanoLC/MS/MSを導入することによって、0.026-50 pmolのNeuGcを定量することに成功した。図1はDMB化NeuAcとDMB化NeuGcのマスクロマトグラムである。本分析法を用いて、10% ウシ胎児血清(FCS)及びヒト血清を含む培地で培養したモデル細胞ヒト骨髄性白血病細胞株HL-60の膜画分由来シアル酸を分析した結果(注入量:細胞2.5 × 10^3個)、それぞれNeuAcの0.4%及び0.1%がNeuGcに置き換わっていることが明らかとなった(表3)。また無血清培地で培養したHL-60細胞中のNeuGcは検出限界(8.6 fmol)以下であった。これは、ヒト血清にはすでにNeuGcが含まれていることを示唆しており、今回得られた結果は、今後NeuGcの有効性・安全性評価、並びに最終製品における規格値設定の必要性を検討する上で、参考になるものと思われる。

2. 細胞の同一性試験

細胞の同一性試験は、製造工程における培養条件の一定性、並びに最終製品の表現型、遺伝型、機能特性及び細胞活性の安定性確認を目的として設定するものである。現在、形態やマルチカラー蛍光*in situ* ハイブリダイゼーションなどの染色体解析が実施されているが、研究レベルでは、マイクロアレイやプロテオミクスなどを基本とした試験法の実行可能性評価も行われている。糖鎖は、培養条件によって変化することが経験的に知られていることから、糖鎖プロファイルが製造工程や最終製品における細胞の同一性指標としてエピジェネティックな表現型の変化も含めて利用できる可能性は高い。我々は、細胞同一性試験法としての糖鎖解析の応用可能性を評価する目的で、HL-60細胞を用いて、培養条件の変化が細胞の糖鎖プロファイルに及ぼす影響を調べた。

はじめに、10% FCSを含む培地で培養したHL-60細胞からN結合型糖鎖を酵素的に切り出し、NaBH4で還元した後、細胞1 × 10^6個相当の糖鎖を用いて、ポジティブイオンFTMS、データ依存的LC/MS/MS～MS/MS/MS/MS、並びにネガティブイオンFTMS、データ依存的LC/MS/MS～MS/MS/MS/MSを行った。データ依存的MS/MS～MS/MS/MS/MSは各スキャンで最も強度の高いイオンを前駆イオンとして行った。図2の青で示す部分は、ポジティブイオンFTMSによって得られたトータルイオンクロマトグラム(TIC)で、主に中性糖鎖とシアル酸結合数の小さい糖鎖のプロファイルを示している。赤で示す部分は、ネガティブイオンFTMSによって得られたTICで、主にシアル酸結合数の大きい糖鎖のプロファイルを表している。主なピークの糖鎖構造は、プロダクトイオンスペクトルから、図2中に示すように推定された。

つぎに、ヒト血清を含む培地、及び無血清培地で培養したHL-60細胞の糖鎖プロファイリングを行った。図3A及び3Bはそれぞれ、ヒト血清及び無血清培地で培養したHL-60細胞由来高マンノース型糖鎖のプロファイルである。無血清培地で培養すると、Man9糖鎖が増加することがわかる。図3C及び3Dは、ポジティブイオンモードで得られたヒト血清及び無血清培地で培養した細胞由来複合型糖鎖のプロファイルである。また、図3E及び3Fはネガティブイオンモードで得られた同糖鎖のプロファイルである。無血清培地ではbisected 2本鎖糖鎖が著しく増加していることが明らかとなった。

今回用いた無血清培地では、細胞の増殖能が低下していたことから、細胞は同一性を失っていたものと判断される。糖鎖プロファイルが全く異なっていたという今回の結果は、糖鎖プロファイリングが細胞の同一性評価法として応用可能であることを示唆していると思われる。厚生労働省はBSE等の問題から、血清は増殖や加工の過程で必須でなければ使用しないこととする通達を出しており、現在、多くの機関で細胞

培養の無血清化が検討されている。一方で、細胞治療薬の安定供給を目指して、様々な研究機関で、自己血清から異種血清への変更も検討されている。細胞中の糖鎖の解析は、細胞の同一性試験だけでなく、最適培養条件のスクリーニングなどにも利用できるかもしれない。また、プロテオグリカンや糖脂質分子等についても、同一性評価指標としての有用性を検討していく必要があるだろう。

3. 細胞純度試験

細胞純度試験は、細胞が期待した特性を有しているか、胎児性細胞への後退、もしくはがん化など望ましくない方向に向かった細胞が混在していないかを評価する試験で、現在は、細胞形態、細胞に特徴的な膜抗原(CD分類)や、細胞が産生する酵素・ケモカイン等の発現解析が中心となっている。糖鎖関連分子としては、SSEA-3、SSEA-4及びCD34のように、すでに優れた細胞表面分化マーカーとして利用されている分子も存在するが、臨床の場で多くの糖鎖関連分子が腫瘍マーカーとして利用されていることを考えると、糖鎖関連分子を細胞純度の指標とした評価法の有用性はより一層増してくると思われる。

ある構造を持つ糖鎖分子の検出には、その構造を特異的に認識する抗体が有用であるが、抗体が入手できないときなど、多段階質量分析(MS^n)が糖鎖の特異的検出法として役立つ場合がある。糖鎖のMS^nでは、例えば、硫酸基 (*m/z* 80)、Lewis a及びx (Le^a, La^x, *m/z* 512)、Sialyl Lewis a及びx (*m/z* 803), HNK-1 (*m/z* 622)、ジシアル酸 (*m/z* 583)のように、糖鎖構造に特徴的なイオン(診断イオン)が生じることがある。これらの診断イオンを利用すると、全糖鎖のプロファイルの中から、関心のある糖鎖構造をもつ糖鎖のマススペクトルだけを選び出すことができる。

図4に、マウス腎臓由来の*N*結合型糖鎖の中からLe^{x}部分構造を持つ糖鎖を選び出した例を示す。糖鎖を2-アミノピリジンで誘導体化した後、

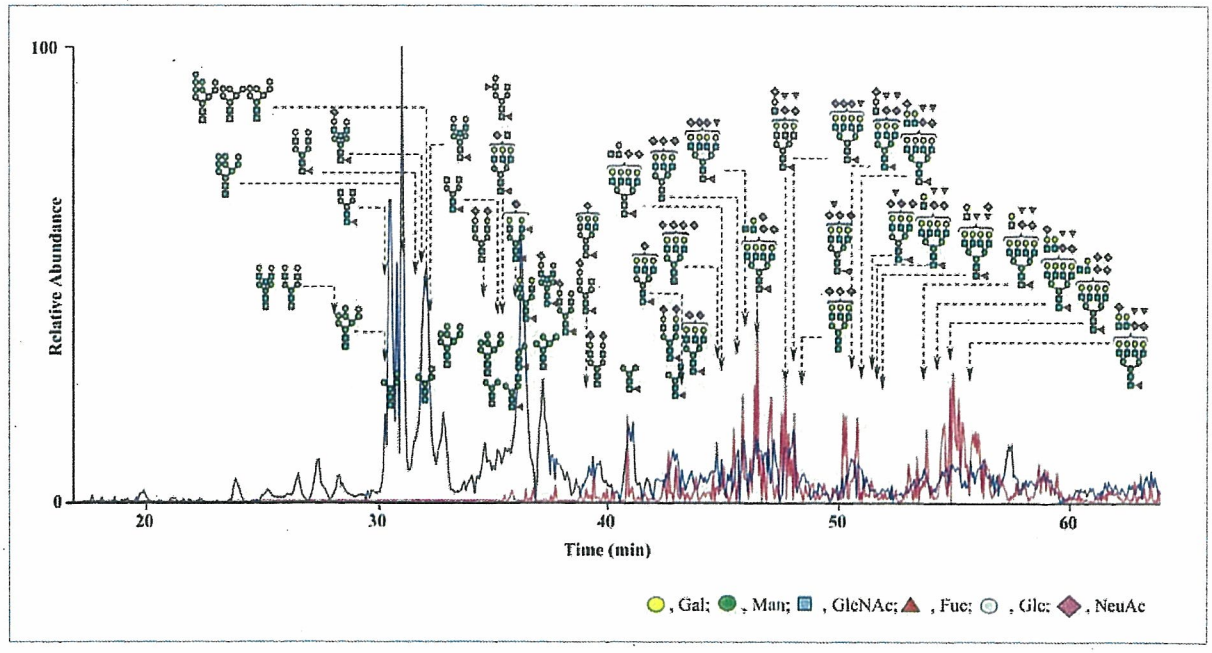

図2. 10 % FCS添加培地で培養したHL-60細胞由来*N*結合型糖鎖のプロファイリング
ポジティブイオンモード(青)、及びネガティブイオンモード(赤) FTMSにより得られたTIC、並びに糖鎖推定構造。
MS: 装置、LTQ-FT; LC: カラム, グラファイトカーボンカラム (5μ, 0.1 × 150mm); A溶媒、2% アセトニトリル/5 mM 酢酸アンモニウム (pH 9.6);B溶媒、 80 % アセトニトリル/5 mM 酢酸アンモニウム (pH 9.6);グラジエント条件、10-40 % B (0-60 min) 及び40-70 % B (60-70 min).

LC/MSで全糖鎖のプロファイリングを行った(図4A)。主な糖鎖分子イオンに対してデータ依存的MS/MSを行い、生じたプロダクトイオンの中から、Le^{x}の構成3糖のナトリウム付加体(*m/z* 534)に相当するイオンを抜き出した(図4B)。つぎに、*m/z* 534のイオンを前駆イオンとしてMS/MS/MSを行い、生成物の中から構成2糖のナトリウム付加体(*m/z* 388)に相当するイオンを選び出し(図4C)、さらにMS/MS/MS/MSを行った。図4Dは、MS/MS/MS/MSで生じたLe^{x}に特徴的な環開裂イオンを抜き出したものである。環開裂を生じた糖鎖のマススペクトルを詳細に解析することによって、腎臓中のLe^{x}の構造を明らかにすることができた[5]。この方法を糖ペプチドに応用すれば、Le^{x}を持つ複数のタンパク質を同定することも可能である。

4. 細胞由来生理活性物質及び細胞由来目的外生理活性物質試験

細胞治療薬から分泌される特定の生理活性物質(例えば、いくつかの製品ではケモカインや増殖因子がその有効性に関わることが明らかになりつつある)が、当該細胞治療薬の効能または効能の本質である場合には、その目的生理活性物質の定量及び特性解析が求められる。目的物質が糖タンパク質である場合は、糖鎖を含む構造特性解析が必要になる。我々は、細胞治療薬が発現する生理活性物質の効率的な構造特性解析法として、電気泳動によるタンパク質の分離とLC/MSによる構造特性解析を検討してきた。

図5は、ラット脳のGPIアンカー型タンパク質の一つを解析した例である。ラット脳膜画分からPIPLC処理によってGPI結合タンパク質を切り出し、SDS-PAGEで分離した(図5A)。はじめに、プロテオミクスの手法で、20-25kDaのバンドに含まれるタンパク質をThy-1と同定した(図5B)。Thy-1は分子内に3箇所の*N*結合

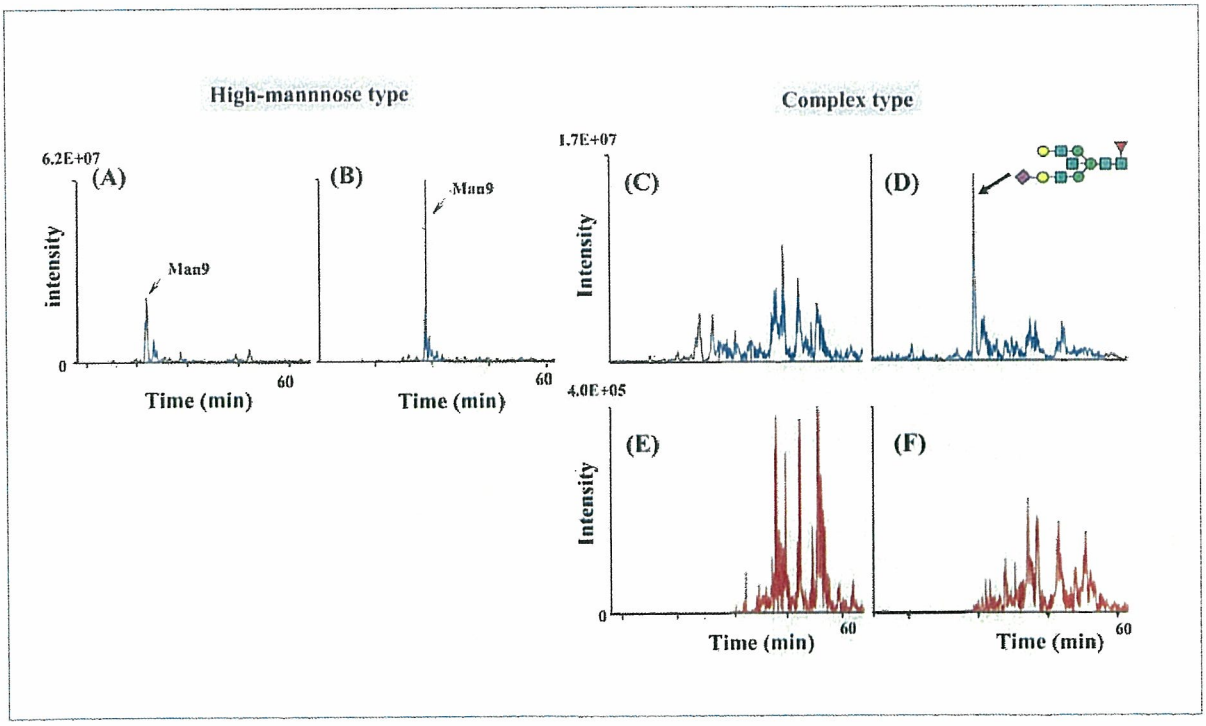

図3. ヒト血清添加培地及び無血清培地で培養したHL-60細胞由来*N*結合型糖鎖のプロフィリング
(A)及び(B)、ポジティブイオンモードで得られた高マンノース型糖鎖のプロファイル; (C)及び(D)、ポジティブイオンモードで得られた複合型糖鎖のプロファイル; (E)及び(F)、ネガティブイオンモードで得られた複合型糖鎖のプロファイル

型糖鎖結合部位をもつ糖タンパク質である。つぎに、ゲル内Nグリカナーゼ消化によりN結合型糖鎖を遊離させ、LC/MS～MS/MS/MS/MSによってThy-1に結合しているN結合型糖鎖を解析した(図5C)。さらに、ゲルから糖タンパク質を抽出した後、トリプシン消化によってペプチド断片とし、LC/MS～MS/MS/MS/MSを用いた部位特異的糖鎖構造解析を行った(図5D)。得られた全マススペクトルの中から糖鎖診断イオン(*m/z* 204, 292, 及び366等)を使って糖ペプチドのプロダクトイオンスペクトルを選び出し、Thy-1の部位特異的糖鎖構造を図6のように推定した[6]。この手法は、複数の糖タンパク質の混合物に対しても応用が可能であり、糖タンパク質ごとの部位特異的糖鎖構造の概略を明らかにすることができる。また、現在この方法は、糖鎖基礎研究としての微量糖タンパク質の構造特性解析にも利用されている。

おわりに

細胞治療薬の品質・安全性評価における糖鎖解析の重要性と、品質試験法としてのLC/MSの応用可能性について示した。BSE問題等に絡む製法変更やバイオ後続品開発が活発に行われている現在、糖鎖構造の変化に着目した製造工程や最終製品の評価は、細胞治療薬だけでなく、バイオ医薬品全般に適用可能な評価手法として再認識されている。バイオ医薬品・細胞治療薬の開発段階から承認審査に至る創薬全般において、糖鎖構造解析技術の開発、糖鎖の機能の解明、及び糖鎖分子マーカー探索研究に対する期待は大きい。

謝辞

シアル酸分析は国立成育医療センター研究所梅澤明弘部長、片桐洋子室長、並びに豊田雅士博士との共同研究です。本研究は、厚生労働科学研究費補助金ゲノム再生医療研究事業、及びヒューマンサイエンス政策創薬総合研究事業の

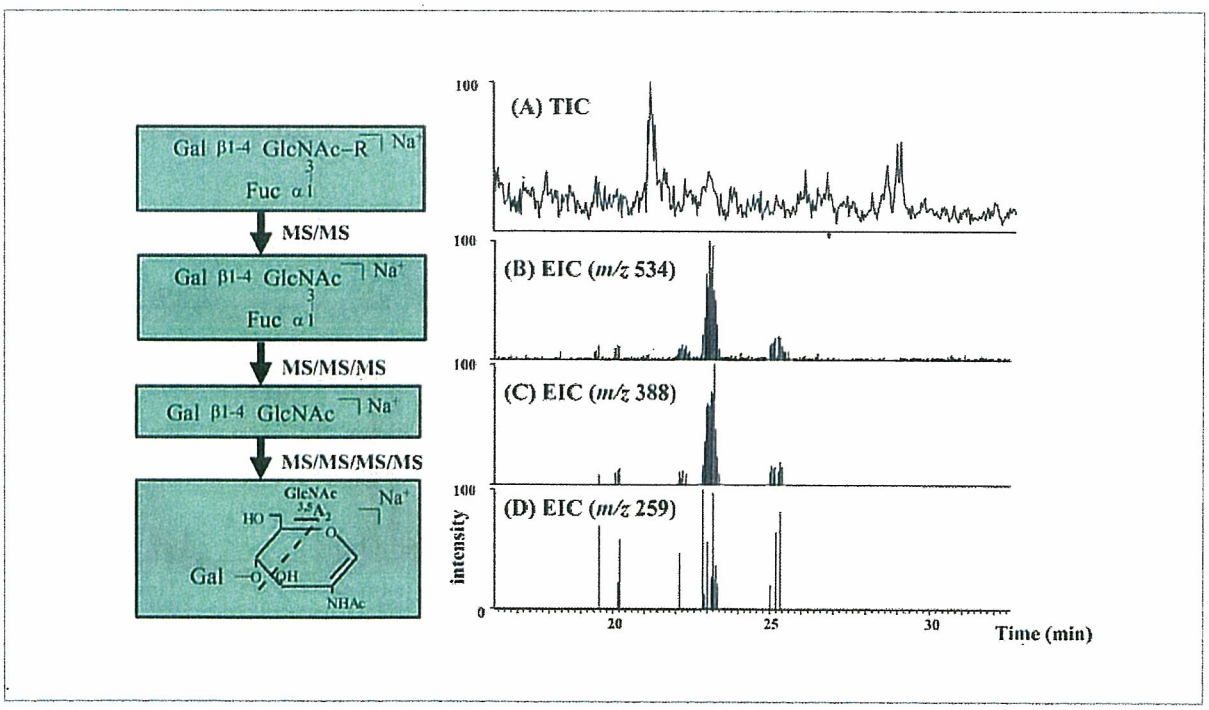

図4. LC/MS/MS/MS/MSによるマウス腎臓由来N結合型Le^{x}糖鎖の特異的検出
(A) TIC; (B) MS/MSで得られたm/z 534のマスクロマトグラム; (C) MS/MS/MSで得られた*m/z* 388のマスクロマトグラム; (D) MS/MS/MS/MSで得られた環開裂フラグメントイオン*m/z* 259のマスクロマトグラム

一環として行われました。本研究を支援してくださいました(財)ヒューマンサイエンス振興財団、キリンビール(株)、中外製薬(株)、(財)化学及び血清療法研究所、アステラス製薬(株)、大日本住友製薬(株)、協和発酵工業(株)、及び厚生労働省に感謝します。

引用文献

1. Higashi, H., Naiki, M., Matuo, S., and Okouchi, K. Antigen of "serum sickness" type of heterophile antibodies in human sera: indentification as gangliosides with N-glycolylneuraminic acid. Biochem Biophys Res Commun 79, 388-95, 1977.
2. Martin, M.J., Muotri, A., Gage, F., and Varki, A. Human embryonic stem cells express an immunogenic nonhuman sialic acid. Nat

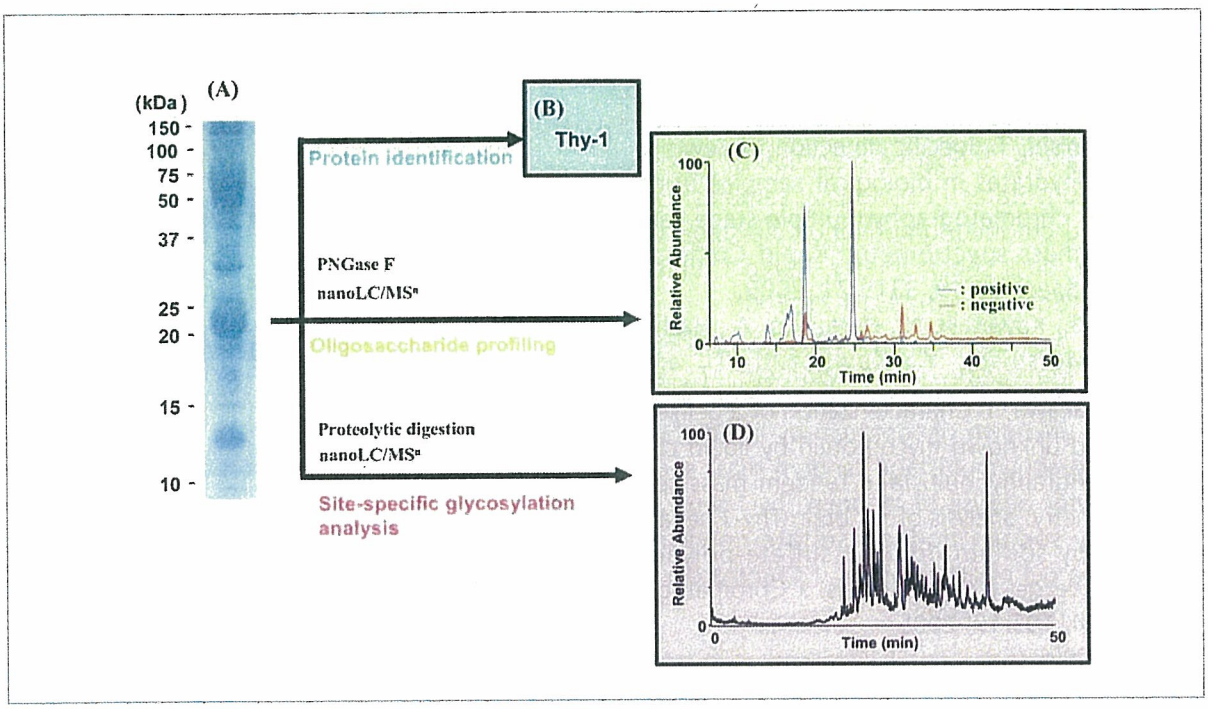

図５．マウス脳由来GPI結合タンパク質の構造特性解析
(A) SDS-PAGE; (B) タンパク質同定; (C) 糖鎖プロファイリング; (D) 部位特異的糖鎖構造解析

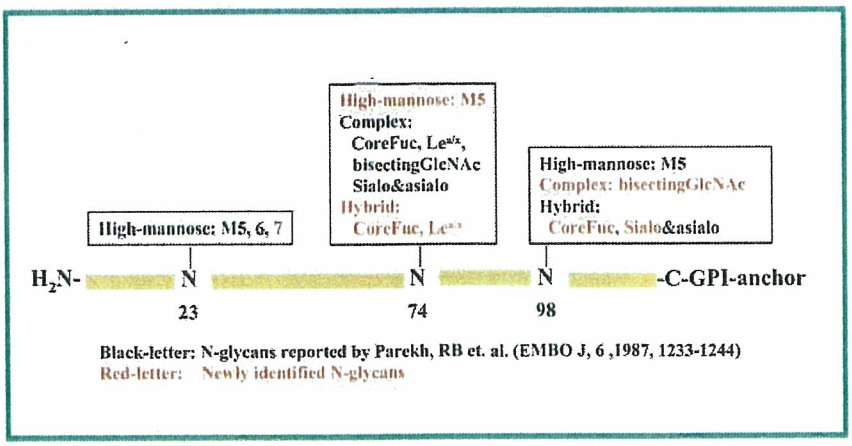

図６．Thy-1の部位特異的糖鎖構造

Med 11, 228-32, 2005.
3. Bardor, M., Nguyen, D.H., Diaz, S., and Varki, A. Mechanism of uptake and incorporation of the non-human sialic acid N-glycolylneuraminic acid into human cells. J Biol Chem 280, 4228-37, 2005.
4. Klein, A., Diaz, S., Ferreira, I., Lamblin, G., Roussel, P., and Manzi, A.E. New sialic acids from biological sources identified by a comprehensive and sensitive approach: liquid chromatography-electrospray ionization-mass spectrometry (LC-ESI-MS) of SIA quinoxalinones. Glycobiology 7, 421-32, 1997.
5. Hashii, N., Kawasaki, N., Itoh, S., Harazono, A., Matsuishi, Y., Hayakawa, T., and Kawanishi, T. Specific detection of Lewis x-carbohydrates in biological samples using liquid chromatography/multiple-stage tandem mass spectrometry. Rapid Commun Mass Spectrom 19, 3315-21, 2005.
6. Itoh, S., Kawasaki, N., Harazono, A., Hashii, N., Matsuishi, Y., Kawanishi, T., and Hayakawa, T. Characterization of a gel-separated unknown glycoprotein by liquid chromatography/multistage tandem mass spectrometry: analysis of rat brain Thy-1 separated by sodium dodecyl sulfate-polyacrylamide gel electrophoresis. J Chromatogr A 1094, 105-17, 2005.

Profile

川崎ナナ
北海道大学薬学部伴義雄教授の下で有機化学を学び、修士課程修了後、厚生労働省国立医薬品食品衛生研究所生物薬品部に入所。1998年から生物薬品部室長。医薬品医療機器総合機構のJAN（医薬品一般名称）専門員及び日本薬局方名称委員及び生物薬品委員を務める。研究テーマはバイオ医薬品及び細胞治療薬の特性解析及び品質・安全性評価技術の開発。現在の目標は医薬品の糖鎖試験法を整備すること。

山口照英
神戸大学理学部大学院（細胞生化学）修了。東京都臨床医学総合研究所で白血球活性酸素生成酵素の生化学に関する研究に従事し、その後国立医薬品食品衛生研究所・生物薬品部でバイオ医薬品の品質・安全性等に関する研究を行う。2002年から遺伝子細胞医薬部長として、遺伝子治療薬や細胞治療薬の品質・有効性に関する基盤研究を実施。2006年から生物薬品部長としてバイオ医薬品の品質・安全性等に関する研究を行っている。

Arteriosclerosis, Thrombosis, and Vascular Biology

Journal of the American Heart Association

American Heart Association®

Learn and Live℠

A Central Role for Nicotinic Cholinergic Regulation of Growth Factor–Induced Endothelial Cell Migration

Martin K.C. Ng, Jenny Wu, Edwin Chang, Bing-yin Wang, Regina Katzenberg-Clark, Akiko Ishii-Watabe and John P. Cooke

Arterioscler. Thromb. Vasc. Biol. 2007;27;106-112; originally published online Nov 2, 2006;
DOI: 10.1161/01.ATV.0000251517.98396.4a
Arteriosclerosis, Thrombosis, and Vascular Biology is published by the American Heart Association. 7272 Greenville Avenue, Dallas, TX 72514
 Print ISSN: 1079-5642. Online ISSN: 1524-4636

A Central Role for Nicotinic Cholinergic Regulation of Growth Factor–Induced Endothelial Cell Migration

Martin K.C. Ng, Jenny Wu, Edwin Chang, Bing-yin Wang, Regina Katzenberg-Clark, Akiko Ishii-Watabe, John P. Cooke

Objective—An endothelial nicotinic acetylcholine receptor (nAChR) participates in atherogenesis and tumorigenesis by promoting neovascularization. To date, the mechanisms of nAChR-mediated angiogenesis and their relationship to angiogenic factors, eg, VEGF and bFGF, are unknown.

Methods and Results—Nicotine induced dose-dependent human microvascular endothelial cell (HMVEC) migration, a key angiogenesis event, to an extent which was equivalent in magnitude to bFGF (10 ng/mL) but less than for VEGF (10 ng/mL). Unexpectedly, nAChR antagonism not only abolished nicotine-induced HMVEC migration but also abolished migration induced by bFGF and attenuated migration induced by VEGF. Transcriptional profiling identified gene expression programs which were concordantly regulated by all 3 angiogens (nicotine, VEGF, and bFGF), a notable feature of which includes corepression of thioredoxin-interacting protein (TXNIP), endogenous inhibitor of the redox regulator thioredoxin. Furthermore, TXNIP repression by all 3 angiogens induced thioredoxin activity. Silencing thioredoxin by small interference RNA abrogated all angiogen-induced migration while silencing TXNIP strongly induced HMVEC migration. Interestingly, nAChR antagonism abrogates growth factor (VEGF and bFGF)–mediated induction of thioredoxin activity.

Conclusions—Nicotine promotes angiogenesis via stimulation of nAChR-dependent endothelial cell migration. Furthermore, growth factor–induced HMVEC migration, a key angiogenesis event, requires nAChR activation—an effect mediated in part by nAChR-dependent regulation of thioredoxin activity. (***Arterioscler Thromb Vasc Biol.* 2007;27: 106-112.**)

Key Words: nicotine ■ angiogenesis ■ endothelium ■ vascular endothelial growth factor ■ fibroblast growth factor

The nicotinic acetylcholine receptor (nAChR) is a pentameric ligand-gated cationic channel.[1] The nAChR was first described in neurons, but has recently been identified in many cell types including endothelial cells (ECs) and vascular smooth muscle cells.[2] Intriguingly, ECs also synthesize and store acetylcholine.[3] Recently, we serendipitously discovered that nAChR activation causes ECs to form capillary tubes in vitro, and promotes angiogenesis in vivo.[4,5]

Pathological as well as physiological forms of angiogenesis are mediated by EC nAChRs. For example, by activating the EC nAChR, nicotine accelerates tumor angiogenesis and tumor growth in a murine Lewis lung cancer model.[4] The acceleration of tumor growth by environmental tobacco smoke is also mediated by nAChR-induced angiogenesis.[6] Furthermore, nAChR activation by nicotine stimulates the neovascularization and progression of atherosclerotic plaque.[4] On the other hand, activation of the nAChR in a murine model of diabetic ulceration enhances wound angiogenesis and healing.[7]

To date, the mechanisms of nAChR-mediated angiogenesis and their relationship to established angiogenic growth factors, such as VEGF and bFGF, are unknown. We therefore sought to study and compare the effects of nAChR activation on EC migration, a key event in angiogenesis, alongside those induced by VEGF or bFGF. In this article, we report an unexpected observation: pharmacological antagonism of the nAChR fully blocks bFGF-induced EC migration, and substantially suppresses the endothelial response to VEGF. Furthermore, by microarray analysis, we identify gene expression programs which are concordantly regulated by nicotine, VEGF, or bFGF, and confirm the role of one of these genes in the cholinergic component of growth factor-induced endothelial cell migration.

Methods

For Methods, please refer to the Data Supplement, available online at http://atvb.ahajournals.org.

Original received April 6, 2006; final version accepted October 16, 2006.

From the Department of Medicine (M.K.C.N., J.W., E.C., B.-y.W., R.K.-C., A.I.-W., J.P.C.), Division of Cardiovascular Medicine, Stanford University School of Medicine, Stanford, Calif.; and the Department of Cardiology (M.K.C.N.), Royal Prince Alfred Hospital, Sydney, NSW, Australia.

M.K.C.N. and J.W. contributed equally to this work

Correspondence to John P. Cooke, Falk Cardiovascular Research Center, Stanford University School of Medicine, 300 Pasteur Drive, Stanford, CA 94305-5406. E-mail john.cooke@stanford.edu

DOI: 10.1161/01.ATV.0000251517.98396.4a

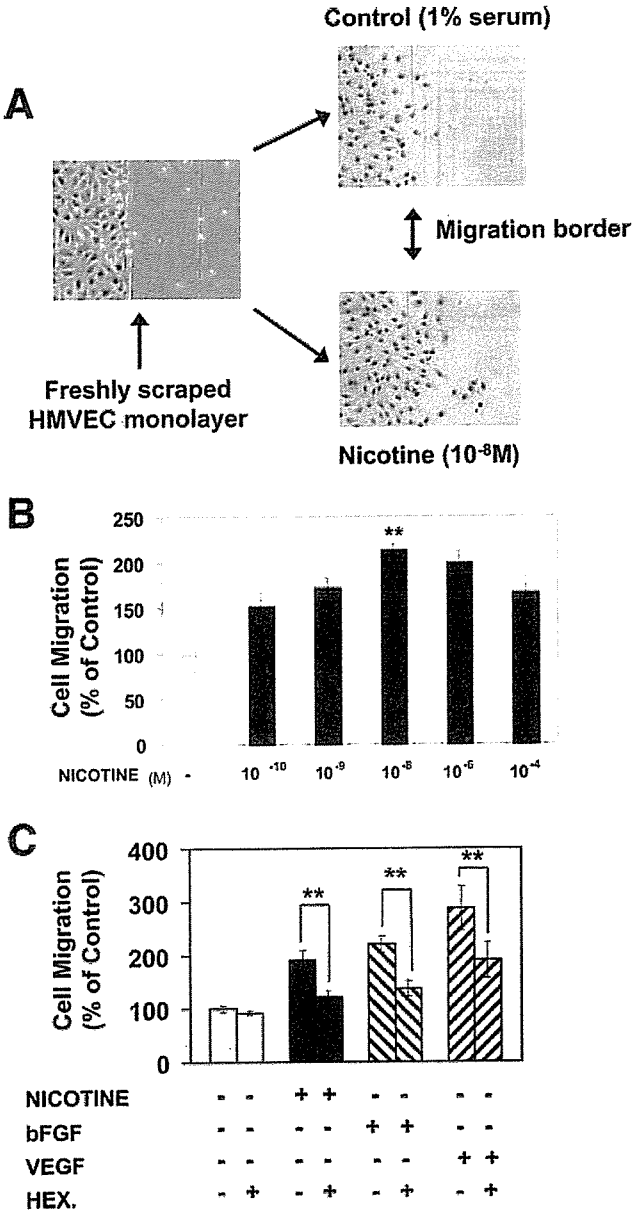

Figure 1. Role of nAChR in human microvascular endothelial cell (HMVEC) migration. A, Representative microphotographs of the HMVEC migration assay: after wounding of the monolayer with a razor blade, HMVECs migrate into the denuded area. B, Nicotine stimulates dose-dependent HMVEC migration which is maximal at a nicotine concentration of 10^{-8} mol/L ($P<0.001$ vs control). C, Effects of hexamethonium (HEX), a nAChR antagonist, on HMVEC migration induced by nicotine (10^{-8} mol/L), VEGF (10 ng/mL), and bFGF (10 ng/mL). Values are expressed as a percentage of migrating cells per high-powered field in vehicle-treated wells. $^{**}P<0.001$.

Results

A Cholinergic Component of Growth Factor–Mediated Endothelial Cell Migration

The effects of nicotine on human microvascular endothelial cell (HMVEC) migration were studied using standard wounding migration assays. Figure 1A depicts typical microphotographs of in vitro HMVEC migration in the presence of vehicle or nicotine. Nicotine stimulated EC migration in a dose-dependent manner with maximal stimulation at 10^{-8} mol/L, producing cell migration that was 216±9% that of vehicle-treated ECs ($P<0.001$ versus control; Figure 1B). Stimulation with VEGF or bFGF also induced EC migration with maximal effects at 10 ng/mL (data not shown). Nicotine-induced EC migration at 10^{-8} mol/L was equivalent in magnitude to that observed for bFGF (10 ng/mL) but less than for VEGF (10 ng/mL; P=NS for nicotine versus bFGF; $P<0.01$ for nicotine versus VEGF; Figure 1C). To further investigate the effects of nAChR-dependent pathways on EC migration, we studied the effect of the nAChR antagonist, hexamethonium (HEX, 10^{-4} mol/L), on EC migration induced by nicotine, VEGF, and bFGF. Hexamethonium abrogated nicotine-induced EC migration (Figure 1C). Unexpectedly, in addition to abolishing NIC-induced EC migration, HEX abolished migration induced by bFGF (P=NS versus control) and reduced migration induced by VEGF ($P<0.01$ for VEGF+HEX versus VEGF alone; Figure 1C). Similar results were observed with the nAChR antagonist, mecamylamine (10^{-6} mol/L; supplemental Figure I). The nAChR-related effect was dose-dependent: in the case of VEGF, cell migration was attenuated by 26±12%, 43±9%, and 52±12% by HEX concentrations of 10^{-8} mol/L, 10^{-6} mol/L, and 10^{-4} mol/L, respectively ($P<0.05$ for trend). Nicotinic receptor activation is known to stimulate EC proliferation.[4] Interestingly, nAChR antagonism also significantly attenuated VEGF- and bFGF-mediated EC proliferation as assessed by bromodeoxyuridine incorporation (supplemental Figure II). The nAChR antagonist-related effects were not the result of cellular toxicity as addition of hexamethonium or mecamylamine alone did not induce cell death as examined via 3-[4,5-dimethylthiazol-2-yl]-2,5-diphenyl tetrazolium bromide (MTT) assays, nor did mecamylamine or hexamethonium induce apoptosis in VEGF- or bFGF-treated cells as assessed by annexin V staining (data not shown).

Previous in vitro and in vivo data have implicated a central role for the α7-nAChR isoform in mediating nAChR-induced neovascularization.[5] Consistent with this, selective inhibition of the α7-nAChR isoform by α-bungarotoxin (10^{-9} mol/L) abrogated nicotine effects (P=NS versus control) and significantly attenuated bFGF and VEGF-induced EC migration by 50±11% and 38±13%, respectively ($P<0.05$ for stimulus versus stimulus + α-bungarotoxin; Figure 2A). We also studied HMVEC α7-nAChR mRNA expression in response to nicotine, VEGF, and bFGF over a 24-hour time course. At 1 hour, nicotine, VEGF, and bFGF all induced >10-fold downregulation of α7-nAChR expression compared with vehicle-treated conditions ($P<0.05$ versus control for all angiogens; Figure 2B). However, by 6 hours, there was significant upregulation of α7-nAChR expression by nicotine (12±0.8-fold), VEGF (11±1.3-fold), and bFGF (4±0.2-fold; $P<0.001$ versus control; Figure 2B). By 24 hours, HMVEC α7-nAChR expression in all conditions had returned to levels similar to control (P=NS versus control). These data suggest that nicotine, VEGF, and bFGF induce acute stimulation of α7-nAChR with subsequent early downregulation of α7-nAChR expression by negative feedback followed by upregulation at 6 hours. These findings are consistent with a role for nAChR in growth factor signaling pathways.

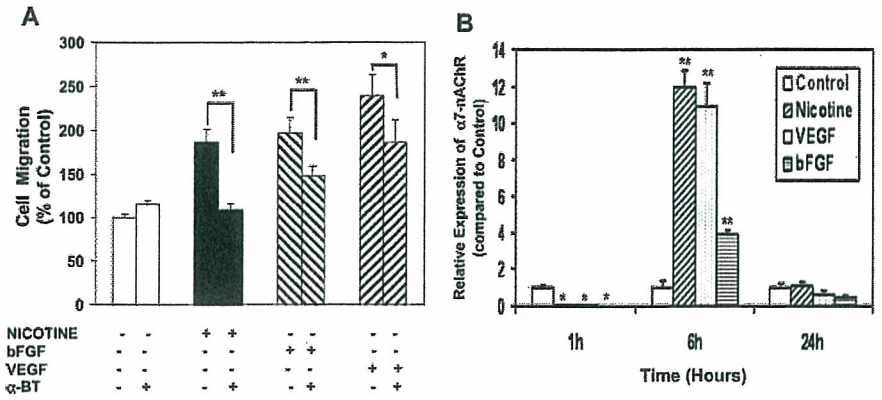

Figure 2. Role of the ∝7-nAChR isoform in growth factor–mediated EC migration. A, Effects of ∝-bungarotoxin (∝-BT), a specific inhibitor of the ∝7-nAChR isoform, on EC migration. Coadministration of ∝-BT (10^{-9} mol/L) abrogated the migragenic effects of nicotine (10^{-8} mol/L; P=NS vs control) and significantly attenuated the effects of bFGF (10 ng/mL) and VEGF (10 ng/mL). B, Effects of nicotine, VEGF, and bFGF on EC ∝7-nAChR expression at 1, 6, and 24 hours as assessed by relative real-time RT-PCR. *P<0.05; **P<0.001 compared with control.

Identification of Shared Transcriptional Responses to Nicotine, bFGF, and VEGF by Microarray Analysis

To further evaluate a cholinergic contribution to growth factor–induced EC migration, and to identify commonly regulated genes that may be required for HMVEC migration, we performed microarray analysis of HMVECs after exposure to nicotine, VEGF, or bFGF. At 24 hours after treatment, each of these stimuli induced profound transcriptional changes in HMVECs (Figure 3), resulting in differential expression of a total of 3072 genes uniquely identified by UniGene, as well as 312 expressed-sequence tags, all of which were represented by 4070 nonredundant cDNA clones. To study relationships between gene expression programs

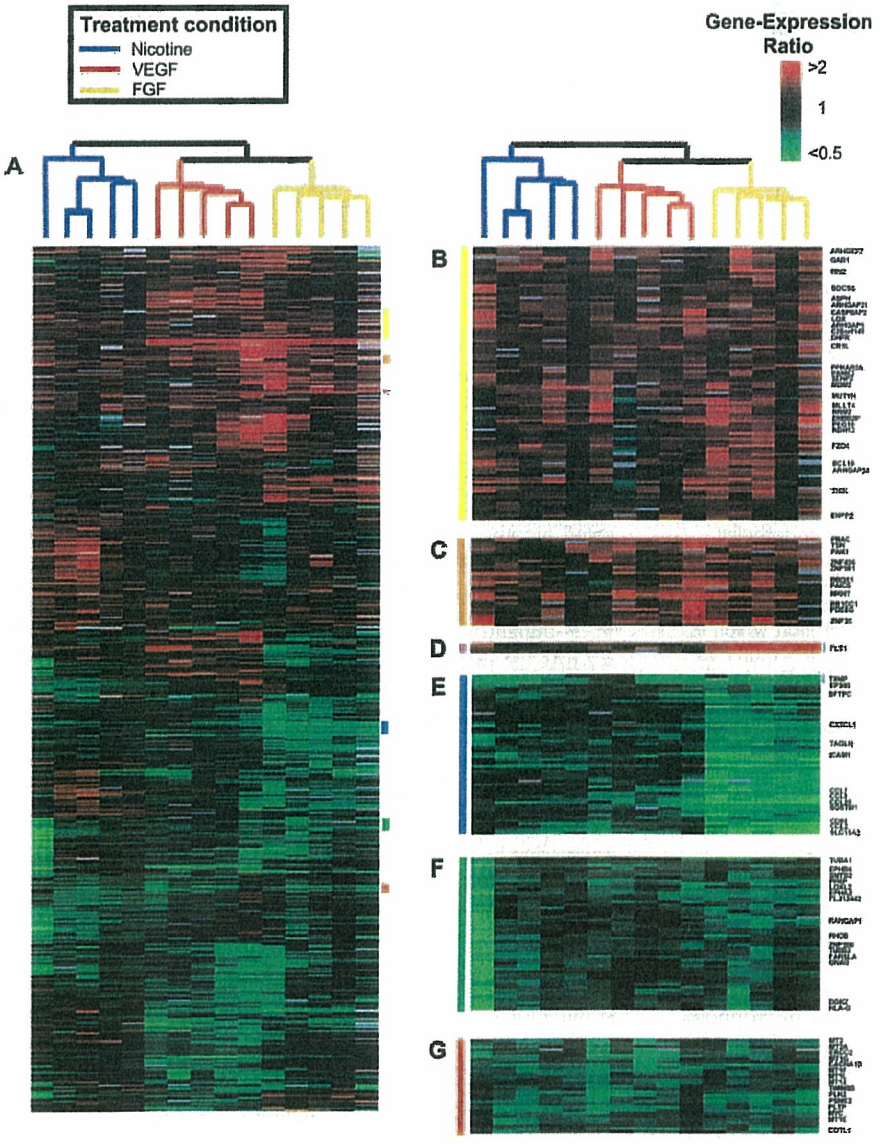

Figure 3. Hierarchical cluster analysis of transcriptional effects of nicotine, VEGF, or bFGF in human microvascular endothelial cells at 24 hours. A, Overview of the two way (genes against conditions) hierarchical cluster of 15 experiments (each condition was studied in quintuplicate) and 4070 nonredundant cDNA clones with significant change in expression at 24 hours. Data from individual elements or genes are represented in rows and experiments in columns. Red and green denote expression levels greater or less, respectively, than control values. Gray denotes technically inadequate or missing data. The intensity of the color reflects the magnitude of the change from baseline. The dendrogram above the matrix represents similarities in patterns of expression between experimental samples. B through G, Zoom boxes of concordantly expressed gene clusters, whose location are indicated by vertical colored bars adjacent to the dendrogram. Owing to space limitations, only genes discussed in the text are indicated by UniGene symbol.

induced by nicotine, VEGF, or bFGF, data for all differentially expressed genes at 24 hours were hierarchically clustered by gene and by array, thereby organizing genes and experimental samples on the basis of similarity of expression patterns (Figure 3A through 3F).[8] The cluster dendrogram shows that all 3 stimuli induced distinct transcriptional signatures which cluster within 3 distinct groups, but there is a closer relationship between the VEGF- and bFGF-induced expression profiles, which cluster together on the same dendrogram branch (Figure 3A).

Within the distinct transcriptional profiles induced by nicotine, VEGF, or bFGF, we identified 6 clusters with concordant gene expression (3 clusters of commonly activated and 3 commonly corepressed genes; Figure 3B through 3F). The characteristics of these clusters provide insights into shared cellular processes that may be requisite for angiogen-induced cell migration. The first activation cluster (Figure 3B), the "migration cluster," was enriched for genes associated with cytokinetic processes including migration-associated G protein signaling (Rho GTPase regulatory proteins and RIN2), integrin binding (ERBB2IP and ADAM9), cell cycle regulation and proliferation (RRM2, MDM2, AHR, MLLT4, and MUTYH), NF-κB activation (BCL10 and CASP8AP2), and migration-associated oxidoreductase activity (LOX and ASPH). Significantly, three Rho GTPase activating proteins (GAPs) including ARHGAP5, ARHGAP21, and ARHGAP24 and one Rho guanine nucleotide exchange factor (GEF), ARHGEF7, were concordantly upregulated in this cluster. Rho GEFs and GAPs, by respectively controlling the activation and inactivation of small Rho GTPases (Cdc42 and Rac), regulate the orchestration of cytoskeletal and adhesive changes during cytokinesis.[9]

A smaller second coactivation cluster (Figure 3C) includes the p21-activated kinase PAK1, an effector for the Rho GTPases Rac and Cdc42, that facilitates cell migration by coordinating formation of new adhesions at the leading edge of the cell with detachment at the trailing edge.[10] Other genes in this activation cluster comprise zinc finger proteins and genes involved in nucleic acid metabolism. Interestingly, all three angiogens induced activation of the VEGF receptor, FLT1, an effect that was stronger for bFGF-treated cells than for nicotine or VEGF (Figure 3D, which contains 3 nonredundant cDNA clones for FLT1). In addition to the coinduction of FLT1 by all three stimuli, we found that several isoforms of nAChR subunits are upregulated by VEGF at 24 hours (supplemental Table I), suggesting other potential synergistic interactions between VEGF and cholinergic signaling pathways.

The first repression cluster (Figure 3E) contains genes that are strongly downregulated by bFGF, many of which are also concordantly repressed by nicotine and VEGF. A dominant theme among concordantly repressed genes is the downregulation of chemokine genes (principally of CC class) involved leukocyte chemotaxis (CCL2, CCL7, CCL8, CCL20, and CX3CL). Another prominent feature is the robust repression of thioredoxin interacting protein (TXNIP) (Figure 3E), a protein that binds and inhibits thioredoxin, a major intracellular antioxidant. Other corepressed genes in this cluster have been implicated in apoptosis (TNFRSF1B, EP300), signal transduction (CD53, SQSTM1), and cell adhesion (ICAM1). The second repression cluster (Figure 3F) included two Ephrin receptors: EPHB4, a marker of venous differentiation and EPHA2, an inhibitor of cell migration which suppresses integrin function. Other genes within this group were associated with tumor suppression, microtubular polymerization, and signal transduction. The striking feature of the third cluster of corepressed genes is a strong enrichment for metallothioneins (MT1E, MT1F, MT1G, MT1L, MT1X, MT2A, and MT3; Figure 3G). Metallothioneins (MTs) comprise a superfamily of small cysteine-rich proteins with high affinity for metal ions and antioxidant activity. By serving as a cellular reservoir for zinc and copper, MTs regulate the function of proteins requiring these metals such as DNA and RNA polymerases, zinc finger transcription factors, and p53.[11] Other genes in this cluster are involved in diverse functions including cell proliferation/apoptosis (MYC, ERCC2), lipid transport (PTLP), calcium ion transport (CACNA1D), and actin binding (COTL1).

In summary, the transcriptional signatures of nicotine, VEGF, and FGF, while distinct, demonstrate many overlapping features. By hierarchical cluster analysis, we have identified a series of shared angiogen-dependent EC transcriptional programs, with implications for understanding shared mechanisms in EC migration/angiogenesis.

Role of Thioredoxin Interacting Protein in the Cholinergic Contribution to Growth Factor–Induced EC Migration

As nAChR antagonism modulates VEGF- and bFGF-dependent EC migration, we hypothesized that some of the transcriptional effects shared by nicotine, VEGF, and bFGF may be nAChR-dependent. Thioredoxin interacting protein (TXNIP), a gene not previously associated with EC migration, was downregulated by all three angiogens. TXNIP is the endogenous inhibitor of thioredoxin. Thioredoxin is a major redox regulator of protein function increasingly implicated in tumorigenesis.[12,13] In microarray data from 3 nonredundant cDNA clones for TXNIP, nicotine, VEGF, and bFGF consistently decreased TXNIP expression—a finding confirmed by RT-PCR, which demonstrated decreased expression by 42±4%, 33±6%, and 26±7% relative to control, respectively ($P<0.001$ for all stimuli; Figure 4A). As in vivo reduction of TXNIP expression in the order of 30% to 40% has been associated with >3-fold increases in thioredoxin activity,[14] we hypothesized that TXNIP downregulation may influence thioredoxin activity and play a role in angiogen-mediated EC migration.

Using a standard assay for thioredoxin activity,[15] we found that addition of nicotine or VEGF induced thioredoxin activity significantly above vehicle-treated cells ($P<0.001$ versus control for all stimuli; Figure 4B). The addition of bFGF induced a less robust ($P<0.05$ versus control) but significant increase in thioredoxin activity (Figure 4B). Notably, coadministration of hexamethonium inhibited nicotine-, VEGF-, or bFGF-induced thioredoxin activity (Figure 4B; $P<0.001$ for each stimulus versus stimulus + hexamethomium). Hexamethonium alone had no significant effect on thioredoxin activity. Consistent with these results, nAChR antagonism abrogated nicotine, VEGF, and bFGF-mediated repression of TXNIP mRNA expression (P=NS versus control for each stimulus + hexamethonium; Figure 4A). Transfection of small interference RNA (siRNA)

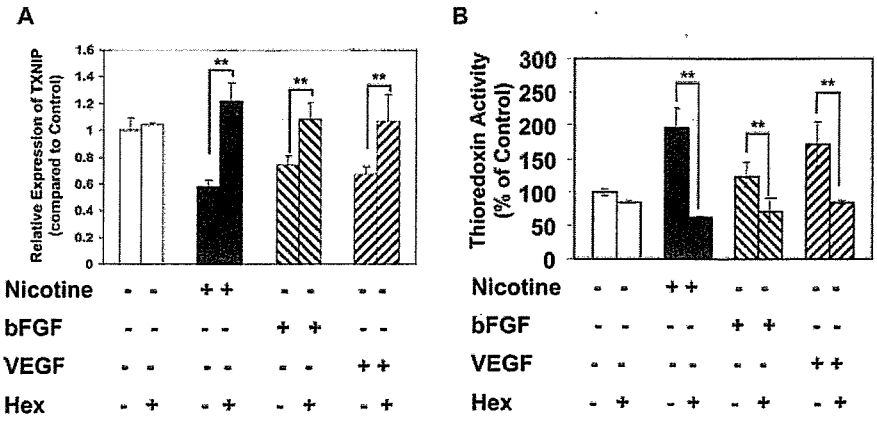

Figure 4. Role of nAChR in growth factor–mediated regulation of TXNIP expression and thioredoxin activity in ECs. Effects of nicotine (10^{-8} mol/L), VEGF (10 ng/mL), and bFGF (10 ng/mL) with/without coadministration of hexamethonium (10^{-4} mol/L) on TXNIP expression (A) and on thioredoxin activity (B) in human microvascular endothelial cells. Values for thioredoxin activity are expressed as a percentage of control (vehicle-treated cells). $^{**}P<0.01$.

against thioredoxin abrogated nicotine-, VEGF-, or bFGF-induced thioredoxin activity and abolished cell migration induced by nicotine, VEGF, or bFGF (P=NS versus control for each stimulus + siRNA; Figure 5A and 5B). Furthermore, in the absence of angiogenic stimuli, siRNA against TXNIP significantly stimulated thioredoxin activity ($P<0.0001$ versus control; Figure 6A) and strongly stimulated HMVEC migration (Figure 6B, $P<0.0001$ versus control). These studies indicate that inhibition of TXNIP by cholinergic or growth factor activation promotes endothelial cell migration, via derepression of thioredoxin activity. Furthermore, VEGF- or bFGF-mediated regulation of TXNIP expression is dependent on activation of nAChR (Figure 4A).

Discussion

We report a cholinergic contribution to growth factor-induced endothelial cell migration. The salient observations are that: (1) activation of nAChR induces EC migration similar in magnitude to that observed for bFGF or VEGF; (2) antagonism of nAChR markedly attenuates the migragenic effects of bFGF or VEGF on ECs; (3) the nAChR-dependent effects of bFGF and VEGF on EC migration are due, in large part, to activation of the ∝7-nAChR isoform; (4) nAChR activation induces a transcriptional profile that has many overlapping features to those induced by bFGF or VEGF, particularly for genes involved in EC migration; (5) downregulation of TXNIP with subsequent induction of thioredoxin activity is shown to be important to the migragenic effects exerted by each of the stimuli; (6) antagonism of the nAChR abrogates VEGF- or bFGF-mediated regulation of TXNIP expression. In toto, our findings identify a novel role for the nicotinic cholinergic pathway in growth factor-mediated EC migration, a critical event in angiogenesis.

Previous studies have demonstrated that ECs synthesize, store, and release acetylcholine[16] and express functional nAChRs.[2] Increasing evidence suggests that such nonneuronal nAChRs are involved in the regulation of vital cell functions, such as mitosis, differentiation, organization of the cytoskeleton, cell–cell contact, locomotion, and migration.[17] Thus, acetylcholine, originally identified as a neurotransmitter, may function as an autocrine factor that modulates migration of endothelial cells. We and others have previously shown that exogenous nicotine, at pathophysiologically relevant concentrations, promotes angiogenesis in a number of in vivo settings, including inflammation, wound healing, ischemia, tumor, and atherosclerosis.[4,7,18] Furthermore, inhibition of nAChR, in the absence of exogenous nicotine, reduces the angiogenic response in vitro and in vivo, indicating that there exists an endogenous cholinergic pathway for angiogenesis.[5] In contrast, recent work has shown that VEGF and FGF, originally identified as angiogenic growth factors, exert neurotrophic effects and promote neurogenesis.[19,20] These and other data suggest that there may be interdependence between "vascular" and "neuronal" factors and processes.

In this study, we found that nicotine induced dose-dependent nAChR-mediated EC migration which was maximal at concentrations consistent with those found in moderate smokers (10^{-8} mol/L). Surprisingly, coadministration of nAChR antagonists, hexamethonium, or mecamylamine, significantly attenuated the migragenic response of ECs to both VEGF and bFGF. Although several nAChR isoforms exist, we have previously identified a principal role for the ∝7-nAChR isoform in nAChR-mediated

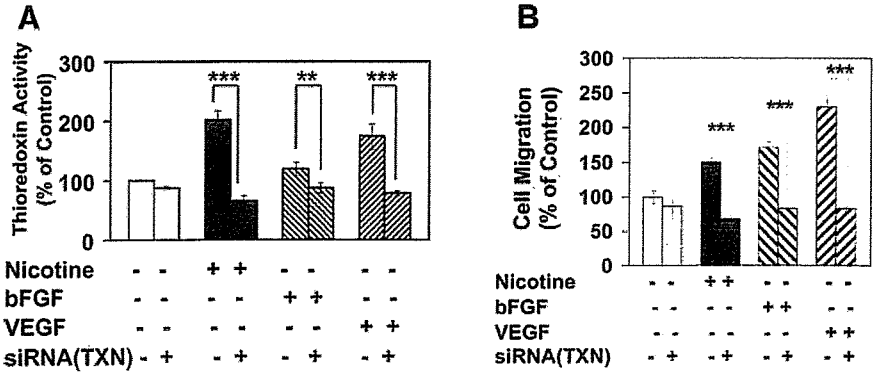

Figure 5. Effects of gene knockdown of thioredoxin by small interference RNA (siRNA) on induction of thioredoxin activity in human microvascular endothelial cells (HMVECs) by nicotine (10^{-8} mol/L), VEGF(10 ng/mL), or bFGF (10 ng/mL) (A) and HMVEC migration induced by nicotine, VEGF, or bFGF (B). Scrambled (randomly arranged) siRNA had no effect on thioredoxin activity or HMVEC migration (data not shown). Values for thioredoxin activity and migration are expressed as a percentage of control (vehicle-treated cells). TXN indicates thioredoxin. $^{**}P$=0.01; $^{***}P<0.001$.

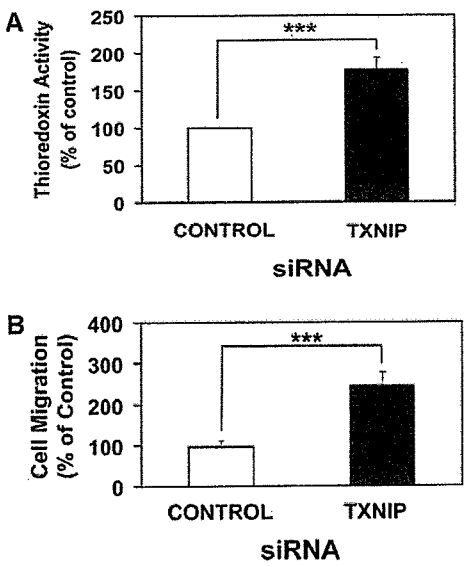

Figure 6. Effects of gene knockdown of thioredoxin interacting protein (TXNIP) by small interference RNA (siRNA) on thioredoxin activity (A) and human microvascular endothelial cell (HMVEC) migration (B). Scrambled (randomly arranged) siRNA had no effect on thioredoxin activity or HMVEC migration (data not shown). Values for thioredoxin activity and migration are expressed as a percentage of control (vehicle-treated cells). ***$P<0.0001$.

angiogenesis in vitro and in vivo.[5] Consistent with these findings, we now find that VEGF and bFGF both induced changes in ∝7-nAChR expression consistent with activation of ∝7-nAChR. Moreover, the ∝7-nAChR selective antagonist, ∝-bungarotoxin, attenuated VEGF and bFGF-induced EC migration to a similar extent as for the nonselective antagonists, hexamethonium, and mecamylamine. These latter findings suggest that nAChR-dependent pathways, particularly via ∝7-nAChR activation, are involved in the modulation of growth factor–induced EC migration.

To study the relationship between nicotine and angiogenic growth factors at a genomic level, microarray analysis was performed after HMVEC exposure to nicotine, VEGF, or bFGF. By hierarchical clustering, we found that each stimulus induced distinct but overlapping transcriptional responses, with concordant gene expression being concentrated within six largely functionally coherent gene clusters. A major functional theme among concordantly expressed genes was the coregulation of cell motility-related processes by all three angiogens. In particular, a "migration" cluster of concordantly activated genes was strongly enriched for genes involved in cytokinetic-related processes such as the Rho GTPase cell motility pathways, integrin binding, cell cycle regulation, and NF-κB activation. Our findings with regard to activation of Rho GTPase pathways by VEGF and bFGF are consistent with previous studies[21] and reinforce the central role of Rho-related regulation of actomyosin cytoskeletal organization EC migration during angiogenesis. We previously demonstrated that nAChR-dependent endothelial tube formation in vitro is dependent on NF-κB activation.[5] The migration cluster included two genes associated with NF-κB activation: BCL10, an important activator of NF-κB downstream of protein kinase C, and CASP8AP2 (aka FLASH), which coordinates downstream NF-κB activity via a TRAF2-dependent pathway.[22] In addition, many genes within the migration cluster have been implicated in oncogenesis (MDM2, ADAM9, BCL10, etc), a finding pathogenetically consistent with the role of angiogenesis in cancer.

The majority of concordantly regulated genes revealed by our microarray analyses have not been previously associated with angiogenesis. These include the p53 inhibitor MDM2 (activated by all three stimuli) and TXNIP, C-C chemokines, and metallothioneins (repressed by all three stimuli). These concordant transcriptional profiles provide further evidence for a cholinergic component of the angiogenic pathways. For example, our findings of coinduction of FLT1 by all three stimuli, and of nAChR subunit induction by VEGF are consistent with interaction between the signaling pathways.

Of the coregulated genes identified by hierarchical clustering, we focused our attention on TXNIP. Originally identified in HL-60 leukemia cells treated with 1,25 dihydroxyvitamin D_3 (and previously known as Vitamin D_3 upregulated protein 1), TXNIP is an endogenous inhibitor of the ubiquitous redox protein thioredoxin.[12] Thioredoxin, a major redox regulator of protein function and signaling via thiol redox control, has been implicated in the regulation of cellular responses to oxidative stress and apoptosis.[23] Thioredoxin selectively regulates the activity of DNA-binding proteins; for example, two transcription factors concordantly regulated by the three stimuli, NF-κB, and p53, require thioredoxin reduction for stimulation of DNA binding.[23,24] Increasing evidence implicates TXNIP and thioredoxin in tumorigenesis. Thioredoxin expression is increased in several human primary cancers, whereas TXNIP is strongly downregulated in human tumor tissues.[13,25] Inhibition of thioredoxin signaling with experimental antitumor agents such as PX-12 (1-methylpropyl 2-imidazolyl disulfide) and pleurotin reduces tumor cell production of HIF-1α and VEGF in vitro and inhibits tumor angiogenesis in vivo.[26] We hypothesized that repression of TXNIP may play a role in mediating growth factor–mediated EC migration.

In the present study, we found that nicotine, VEGF, and bFGF stimulated thioredoxin activity—a finding consistent with their common suppression of TXNIP. Gene knockdown of thioredoxin by siRNA reversed the effect of growth factor stimulation and abrogated the effect of nicotine, VEGF, or bFGF on EC migration. These findings are consistent with a critical role for thioredoxin in mediating growth factor–induced EC migration. Interestingly, the increase in thioredoxin activty induced by each of the three stimuli could be blocked by nAChR antagonism. Finally, gene knockdown of TXNIP alone, without addition of growth factors, induced EC migration. Our findings indicate that TXNIP, by regulating of thioredoxin activity, may play an important role in angiogenesis mediated by growth factor receptors or nAChRs. The mechanism whereby thioredoxin mediates EC migration is poorly understood but may involve stimulation of hypoxia-inducible factor-1α (HIF-1α), a transcription factor that plays a central role in mediating the angiogenic response to hypoxia. Overexpression of thioredoxin in a variety of malignant cells has been shown to induce HIF-1α expression and VEGF production.[27] Induction of HIF-1α in human endothelial cells upregulates the expression of multiple angiogenic factors including the angiopoietins which are potent stimulators of cell migration via Tie-2 signal transduction pathways.[28] Moreover, as cellular redox state is an important determinant of Rho

GTPase activity, it is possible that thioredoxin may play a role in Rho-mediated cytoskeletal remodelling during cell migration.[29]

In summary, our data show that activation of nicotinic acetylcholine receptors (nAChRs) induces endothelial cell migration. Furthermore, growth factor (VEGF and bFGF)–induced endothelial cell migration involves nAChR activation. By transcriptional profiling we have identified convergent genomic responses of ECs to nicotine, VEGF, and bFGF. Identification of concordantly regulated genes may provide novel insights into molecular processes mediating EC migration and angiogenesis. Indeed, using this approach we found that TXNIP, by regulating thioredoxin activity, is centrally involved in nAChR-mediated EC migration. Our studies provide evidence for a cholinergic contribution to growth factor-induced EC migration. The nAChRs may play an important role in growth factor-induced angiogenesis, and thus may be a target for therapeutic modulation in disorders of pathological or insufficient angiogenesis.

Acknowledgments

We thank Mary Gerritsen, PhD, and Ken Kengatharan, PhD for scientific and editorial comments.

Sources of Funding

Akiko Ishii-Watabe is supported by the Japanese Health Sciences Foundation. Martin K.C. Ng is supported by the National Health and Medical Research Council of Australia. This study was supported by grants from the National Institutes of Health (R01 HL-63685; RO1 HL-75774; R01 CA098303 and P01 AG18784; and PO1AI50153); Philip Morris USA Inc; and the Tobacco Related Disease Research Program (11RT-0147).

Disclosures

Dr Cooke holds equity in Athenagen Inc, which has licensed Stanford University patents for the use of nAChR agonists and antagonists for disorders of angiogenesis. Dr Cooke is an inventor on these patents, and receives royalties from the licenses. A patent is being filed based upon the intellectual property described in this manuscript that may benefit J.P.C., M.K.C.N., E.C., and J.W.

References

1. Lindstrom J. Nicotinic acetylcholine receptors in health and disease. *Mol Neurobiol.* 1997;15:193–222.
2. Macklin KD, Maus AD, Pereira EF, Albuquerque EX, Conti-Fine BM. Human vascular endothelial cells express functional nicotinic acetylcholine receptors. *J Pharmacol Exp Ther.* 1998;287:435–439.
3. Parnavelas JG, Kelly W, Burnstock G. Ultrastructural localization of choline acetyltransferase in vascular endothelial cells in rat brain. *Nature.* 1985;316:724–725.
4. Heeschen C, Jang JJ, Weis M, Pathak A, Kaji S, Hu RS, Tsao PS, Johnson FL, Cooke JP. Nicotine stimulates angiogenesis and promotes tumor growth and atherosclerosis. *Nat Med.* 2001;7:833–839.
5. Heeschen C, Weis M, Aicher A, Dimmeler S, Cooke JP. A novel angiogenic pathway mediated by non-neuronal nicotinic acetylcholine receptors. *J Clin Invest.* 2002;110:527–536.
6. Zhu BQ, Heeschen C, Sievers RE, Karliner JS, Parmley WW, Glantz SA, Cooke JP. Second hand smoke stimulates tumor angiogenesis and growth. *Cancer Cell.* 2003;4:191–196.
7. Jacobi J, Jang J, Sundram U, Dayoub H, Fajardo LF, Cooke JP. Nicotine accelerates angiogenesis and wound healing in genetically diabetic mice. *Am J Pathol.* 2002;161:97–104.
8. Eisen MB, Spellman PT, Brown PO, Botstein D. Cluster analysis and display of genome-wide expression patterns. *Proc Natl Acad Sci U S A.* 1998;95:14863–14868.
9. Ridley A, Schwartz M, Burridge K, Firtel R, Ginsberg M, Borisy G, Parsons J, Horwitz A. Cell migration: integrating signals from front to back. *Science.* 2003;302:1704–1709.
10. Kiosses W, Daniels R, Otey C, Bokoch G, Schwartz M. A role for p21-activated kinase in endothelial cell migration. *J Cell Biol.* 1999;147:831–844.
11. Henkel G, Krebs B. Metallothioneins: zinc, cadmium, mercury, and copper thiolates and selenolates mimicking protein active site features - structural aspects and biological implications. *Chem Rev.* 2004;104:801–824.
12. Nishiyama A, Matsui M, Iwata S, Hirota K, Masutani H, Nakamura H, Takagi Y, Sono H, Gon Y, Yodoi J. Identification of thioredoxin-binding protein-2/vitamin D(3) up-regulated protein 1 as a negative regulator of thioredoxin function and expression. *J Biol Chem.* 1999;274:21645–21650.
13. Baker A, Payne CM, Briehl MM, Powis G. Thioredoxin, a gene found overexpressed in human cancer, inhibits apoptosis *in vitro* and *in vivo*. *Cancer Res.* 1997;57:5162–5167.
14. Yoshioka J, Schulze PC, Cupesi M, Sylvan JD, MacGillivray C, Gannon J, Huang H, Lee RT. Thioredoxin-interacting protein controls cardiac hypertrophy through regulation of thioredoxin activity. *Circulation.* 2004;109:2581–2586.
15. Wang YG, De Keulenaer GW, Lee RT. Vitamin D(3)-up-regulated protein-1 is a stress-responsive gene that regulates cardiomyocyte viability through interaction with thioredoxin. *J Biol Chem.* 2002;277:26496–26500.
16. Milner P, Kirkpatrick KA, Ralevic V, Toothill V, Pearson J, Burnstock G. Endothelial cells cultured from human umbilical vein release ATP, substance P and acetylcholine in response to increased flow. *Proc Biol Sci.* 1990;241:245–248.
17. Wessler I, Kirkpatrick CJ, Racke K. The cholinergic 'pitfall': acetylcholine, a universal cell molecule in biological systems, including humans. *Clin Exp Pharmacol Physiol.* 1999;26:198–205.
18. Natori T, Sata M, Washida M, Hirata Y, Nagai R, Makuuchi M. Nicotine enhances neovascularization and promotes tumor growth. *Mol Cells.* 2003;16:143–146.
19. Jin K, Zhu Y, Sun Y, Mao XO, Xie L, Greenberg DA. Vascular endothelial growth factor (VEGF) stimulates neurogenesis in vitro and in vivo. *Proc Natl Acad Sci U S A.* 2002;99:11946–11950.
20. Yoshimura S, Takagi Y, Harada J, Teramoto T, Thomas SS, Waeber C, Bakowska JC, Breakefield XO, Moskowitz MA. FGF-2 regulation of neurogenesis in adult hippocampus after brain injury. *Proc Natl Acad Sci U S A.* 2001;10:5874–5879.
21. Soga N, Namba N, McAllister S, Cornelius L, Teitelbaum S, Dowdy S, Kawamura J, Hruska K. Rho family GTPases regulate VEGF-stimulated endothelial cell motility. *Exp Cell Res.* 2001;269:73–87.
22. Choi Y, Kim K, Kim H, Hong G, Kwon Y, Chung C, Park Y, Shen Z, Kim B, Lee S, Jung Y. FLASH coordinates NF-kappa B activity via TRAF2. *J Biol Chem.* 2001;276:25073–25077.
23. Yamawaki H, Haendeler J, Berk BC. Thioredoxin. A key regulator of cardiovascular homeostasis. *Circ Res.* 2003;93:1029–1033.
24. Ueno M, Masutani H, Arai RJ, Yamauchi A, Hirota K, Sakai T, Inamoto T, Yamaoka Y, Yodoi J, Nikaido T. Thioredoxin-dependent redox regulation of p53-mediated p21 activation. *J Biol Chem.* 1999;274:35809–35815.
25. Kakolyris S, Giatromanolaki A, Koukourakis M, Powis G, Souglakos J, Sivridis E, Georgoulias V, Gatter KC, Harris AL. Thioredoxin expression is associated with lymph node status and prognosis in early operable non-small cell lung cancer. *Clin Cancer Res.* 2001;7:3087–3091.
26. Welsh SJ, Williams RR, Birmingham A, Newman DJ, Kirkpatrick DL, Powis G. The thioredoxin redox inhibitors 1-methylpropyl 2-imidazolyl disulfide and pleurotin inhibit hypoxia-induced factor 1alpha and vascular endothelial growth factor formation. *Mol Cancer Ther.* 2003;2:235–243.
27. Welsh SJ, Bellamy WT, Briehl MM, Powis G. The redox protein thioredoxin-1 (Trx-1) increases hypoxia-inducible factor 1alpha protein expression: Trx-1 overexpression results in increased vascular endothelial growth factor production and enhanced tumor angiogenesis. *Cancer Res.* 2002;62:5089–5095.
28. Yamakawa M, Liu LX, Date T, Belanger AJ, Vincent KA, Akita GY, Kuriyama T, Cheng SH, Gregory RJ, Jiang C. Hypoxia-inducible factor-1 mediates activation of cultured vascular endothelial cells by inducing multiple angiogenic factors. *Circ Res.* 2003;93:664–673.
29. Nimnual AS, Taylor LJ, Bar-Sagi D. Redox-dependent downregulation of Rho by Rac. *Nat Cell Biol.* 2003;5:236–241.

Available online at www.sciencedirect.com
SCIENCE DIRECT®
Analytical Biochemistry 348 (2006) 259–268
ANALYTICAL BIOCHEMISTRY
www.elsevier.com/locate/yabio

Site-specific N-glycosylation analysis of human plasma ceruloplasmin using liquid chromatography with electrospray ionization tandem mass spectrometry

Akira Harazono *, Nana Kawasaki, Satsuki Itoh, Noritaka Hashii, Akiko Ishii-Watabe, Toru Kawanishi, Takao Hayakawa

National Institute of Health Sciences, Division of Biological Chemistry and Biologicals, 1-18-1 Kami-yoga, Setagaya-Ku, Tokyo 158-8501, Japan

Received 8 June 2005
Available online 10 November 2005

Abstract

Ceruloplasmin has ferroxidase activity and plays an essential role in iron metabolism. In this study, a site-specific glycosylation analysis of human ceruloplasmin (CP) was carried out using reversed-phase high-performance liquid chromatography with electrospray ionization tandem mass spectrometry (LC-ESI-MS/MS). A tryptic digest of carboxymethylated CP was subjected to LC-ESI-MS/MS. Product ion spectra acquired data-dependently were used for both distinction of the glycopeptides from the peptides using the carbohydrate B-ions, such as *m/z* 204 (HexNAc) and *m/z* 366 (HexHexNAc), and identification of the peptide moiety of the glycopeptide based on the presence of the b- and y-series ions derived from the peptide. Oligosaccharide composition was deduced from the molecular weight calculated from the observed mass of the glycopeptide and theoretical mass of the peptide. Of the seven potential N-glycosylation sites, four (Asn119, Asn339, Asn378, and Asn743) were occupied by a sialylated biantennary or triantennary oligosaccharide with fucose residues (0, 1, or 2). A small amount of sialylated tetraantennary oligosaccharide was detected. Exoglycosidase digestion suggested that fucose residues were linked to reducing end GlcNAc in biantennary oligosaccharides and to reducing end and/or α1–3 to outer arms GlcNAc in triantennary oligosaccharides and that roughly one of the antennas in triantennary oligosaccharides was α2–3 sialylated and occasionally α1–3 fucosylated at GlcNAc.

Keywords: Ceruloplasmin; Glycopeptide; Liquid chromatography-electrospray tandem mass spectrometry; Product ion spectrum; Exoglycosidase digestion

Ceruloplasmin (CP)[1] is a blue copper serum glycoprotein synthesized in the liver. CP has ferroxidase activity and plays an essential role in iron metabolism [1–4]. The primary structure of human CP has been determined by amino acid sequencing, and it is composed of a single polypeptide chain of 1046 amino acid residues [5]. The amino acid sequence was confirmed from complete cDNA sequence [6]. The major oligosaccharides in human CP were reported to be sialylated bi- and triantennary structures with or without a fucose residue [7,8]. Although four N-glycosylation sites (Asn119, Asn339, Asn378, and Asn743) were identified among seven potential sites [9], the heterogeneity of oligosaccharides was still unknown at each glycosylation site. CP is an acute phase reactant, and the serum concentration increases during inflammation, infection, and trauma [10]. It is known that the patterns of glycosylation are changed by inflammatory cytokines [11]. Several studies have reported that CP is a good diagnostic marker of solid malignant tumors [12,13] and that the CP glycoform might

* Corresponding author. Fax: +81 3 3700 9084.
E-mail address: harazono@nihs.go.jp (A. Harazono).

[1] *Abbreviations used:* CP, ceruloplasmin; LC-ESI-MS, liquid chromatography with electrospray ionization mass spectrometry; Hex, hexose; HexNAc, *N*-acetylhexosamine; LC-ESI-MS/MS, liquid chromatography with electrospray ionization tandem mass spectrometry; EDTA, ethylenediaminetetraacetic acid; TFA, trifluoroacetic acid; Q-TOF, quadrupole time-of-flight; TIC, total ion chromatogram; NeuAc, *N*-acetylneuraminic acid; GlcNAc, *N*-acetylglucosamine; Fuc, fucose.

0003-2697/$ - see front matter © 2005 Elsevier Inc. All rights reserved.
doi:10.1016/j.ab.2005.10.036

be a valuable supplement [12]. Thus, it is important to conduct a site-specific glycosylation analysis of normal human CP.

One of the most effective techniques for determining the site-specific carbohydrate heterogeneity of glycoproteins is the mass spectrometric peptide mapping of proteolytic fragments of glycoproteins by liquid chromatography with electrospray ionization mass spectrometry (LC-ESI-MS) [14–19]. The specific detection of glycopeptides in a complex peptide mixture is generally achieved by monitoring specific carbohydrate fragment ions such as *m/z* 204 (HexNAc) and *m/z* 366 (HexHexNAc) produced by cone voltage fragmentation or by precursor ion scanning [15–19]. Because product ion spectra of glycopeptides show high abundant carbohydrate fragment ions and low abundant b- and y-series fragment ions derived from the peptide backbone [20,21], product ion spectra acquired data-dependently in liquid chromatography with electrospray ionization tandem mass spectrometry (LC-ESI-MS/MS) can be used for both the selection from the peptides and the identification of the glycopeptides [22]. MS in combination with specific exoglycosidase digestions allows us to obtain the site-specific information on anomericity and linkage of glycans [23]. In the current study, we conducted a site-specific glycosylation analysis of human CP and successfully determined glycosylation status and glycosylation profile at each N-glycosylation site.

Materials and methods

Materials

Acetonitrile, formic acid, and guanidine hydrochloride were purchased from Wako Pure Chemicals Industries (Osaka, Japan). Purified human CP was purchased from Calbiochem (San Diego, CA, USA). Modified trypsin was purchased from Promega (Madison, WI, USA). α2–3 Neuraminidase (EC 3.2.1.18) of *Macrobdella decora*, a recombinant form, and α1–3,4 fucosidase (EC 3.2.1.51) from *Xanthomonas* sp. were purchased from Calbiochem. α2–3,6,8,9 Neuraminidase (EC 3.2.1.18) of *Arthrobacter ureafaciens*, a recombinant form, and β1–4 galactosidase (EC 3.2.1.23) were purchased from Sigma Chemical (St. Louis, MO, USA). The water used was obtained from a Milli-Q water system (Millipore, Bedford, MA, USA). All other reagents were of the highest quality available.

Reduction and S-carboxymethylation of CP

CP (100 μg) was dissolved in 270 μl of 0.5 M Tris–HCl buffer (pH 8.5) that contained 8 M guanidine hydrochloride and 5 mM ethylenediaminetetraacetic acid (EDTA). After the addition of 2 μl of 2-mercaptoethanol, the mixture was incubated for 2 h at 40 °C. Then 5.67 mg of monoiodoacetic acid was added, and the resulting mixture was incubated for 2 h at 40 °C in the dark. The reaction mixture was applied to a PD-10 column (Amersham Biosciences, Uppsala, Sweden) to remove the reagents, and the eluate was lyophilized.

Trypsin digestion of CP

Reduced and carboxymethylated CP was redissolved in 100 μl of 0.1 M Tris–HCl buffer (pH 8.0). An aliquot of 1 μl of trypsin prepared as 1 μg/μl was added to 50 μl of CP solution (1:50, w/w), and the mixture was incubated for 16 h at 37 °C. The enzyme digestion was stopped by storing at −20 °C before analysis.

HPLC of tryptic digest of CP

Tryptic digests (0.2 and 0.4 μg) of human CP were analyzed by LC-ESI-MS/MS to identify the peptides and glycopeptides, respectively. HPLC was performed on a Paradigm MS 4 (Michrome BioResources, Auburn, CA, USA) equipped with a Magic C18 column (0.2 μ, 50 mm, Michrome BioResources). The eluents consisted of water containing 2% (v/v) acetonitrile and 0.1% (v/v) formic acid (pump A) and 90% acetonitrile and 0.1% formic acid (pump B). Trypsin-digested samples were loaded onto a microtrap (peptide captrap, Michrom BioResources). After a wash with 15 μl H_2O/CH_3CN (98:2) with 0.1% trifluoroacetic acid (TFA), the trapping column was switched into line with the column. Samples were eluted with 5% of B for 10 min, followed by a linear gradient from 5 to 65% of B in 60 min at a flow rate of 2 μl/min.

ESI-Q-TOF-MS/MS

Mass spectrometric analyses were performed using a quadrupole time-of-flight (Q-TOF) mass spectrometer (QSTAR Pulsar, MDS Sciex, Toronto, Canada) equipped with a nano-electrospray ion source. The mass spectrometer was operated in the positive ion mode. The nanospray voltage was set at 2500 V. Mass spectra were acquired at *m/z* 400–2000 or *m/z* 1000–2000 for MS analysis and at *m/z* 100–2000 for MS/MS analysis. After every regular MS acquisition, two MS/MS acquisitions against top two of the multiply charged molecular ions were performed (data-dependent acquisition). The precursor ions with the same *m/z* as acquired previously were excluded for 120 s. The collision energy was varied between 30 and 80 eV depending on the size and charge of the molecular ion. Accumulation times for the spectra were 1.0 and 2.0 s for MS and MS/MS, respectively. All peaks were resolved monoisotopically.

Tandem MS/MS data from LC-ESI-MS/MS runs were submitted to the search engine Mascot to identify the tryptic peptides of CP. One missed cleavage was allowed, and tolerances of 2.0 and 0.8 u mass were used for precursor and product ions, respectively. From the data for LC-ESI-MS/MS at *m/z* 1000–2000, glycopeptide precursor ions were selected manually based on the presence of oligosaccharide oxonium ions such as *m/z* 204 (HexNAc) and *m/z* 366 (HexHexNAc). The glycopeptide ions were assigned based on